

Nanoscale

Accepted Manuscript



This is an *Accepted Manuscript*, which has been through the Royal Society of Chemistry peer review process and has been accepted for publication.

Accepted Manuscripts are published online shortly after acceptance, before technical editing, formatting and proof reading. Using this free service, authors can make their results available to the community, in citable form, before we publish the edited article. We will replace this *Accepted Manuscript* with the edited and formatted *Advance Article* as soon as it is available.

You can find more information about *Accepted Manuscripts* in the [Information for Authors](#).

Please note that technical editing may introduce minor changes to the text and/or graphics, which may alter content. The journal's standard [Terms & Conditions](#) and the [Ethical guidelines](#) still apply. In no event shall the Royal Society of Chemistry be held responsible for any errors or omissions in this *Accepted Manuscript* or any consequences arising from the use of any information it contains.

Controlling Enzymatic Activity and Kinetics in Swollen Mesophases by Physical Nano-Confinement

*Wenjie Sun, Jijo J. Vallooran, Alexandru Zabara, Raffaele Mezzenga**

ETH Zurich, Food and Soft Materials Science, Institute of Food, Nutrition & Health,

Department of Health Science and Technology, Schmelzbergstrasse 9,

CH-8092 Zurich, Switzerland

*Corresponding author: email: raffaele.mezzenga@hest.ethz.ch

Abstract

Bicontinuous lipid cubic mesophases are widely investigated as hosting matrices for functional enzymes to build biosensors and bio-devices due to their unique structural characteristics. However, the enzymatic activity within standard mesophases (*in-meso*) is severely hindered by the relatively small diameter of the mesophase aqueous channels, which provide only limited space for enzymes, and restrict them into a highly confined environment. We show that the enzymatic activity of a model enzyme, Horseradish Peroxidase (HRP), can be accurately controlled by relaxing its confinement within the cubic phases' water channels, when the aqueous channel diameters are systematically swollen with varying amount of hydration-enhancing sugar ester.

The *in-meso* activity and kinetics of HRP is then systematically investigated by UV-vis spectroscopy, as a function of the size of aqueous mesophase channels. The enzymatic activity of HRP increases with the swelling of the water channels. In swollen mesophases with water channel diameter larger than HRP size, the enzymatic activity is more than double than that measured in standard mesophases, approaching again the enzymatic activity of free HRP in bulk water. We also show that the physically-entrapped enzymes in the mesophases exhibit a restricted-diffusion-induced initial lag period and report the first observation of *in-meso* enzymatic kinetics significantly deviating from the normal Michaelis-Menten behaviour observed in free solutions, with deviations vanishing when enzyme confinement is released by swelling the mesophase.

Introduction

Lipid-based bicontinuous cubic phases are excellent hosting matrices for the encapsulation and sustained release of bioactive ingredients,¹⁻⁶ protein crystallization⁷⁻⁹ and material templates,¹⁰ as well as for biosensing, environmental and biomedical detection.¹¹⁻¹⁶ This wide-ranging applicability can be directly attributed to their unique topological architecture, where a three-dimensional periodic lipidic bilayer with a zero mean curvature at each point (following triply periodical minimal surfaces) separates two sets of interpenetrating but non-communicating water channels. The dual polar/nonpolar nature of these mesophases allows for a variety of amphiphilic,¹ hydrophilic²⁻⁴ and hydrophobic bioactives⁵ to be successfully incorporated.

Biosensing based on gel-like matrices (hydrogels,¹⁷ sol-gels^{18, 19} and mesophases¹¹⁻¹⁶) has been widely explored in the past decades. There are several distinct strategies for biosensing, each differentiated by the various methods employed to follow the changes in signal during the specific enzymatic reactions (i.e. optical biosensing and electrochemical biosensing). Optical biosensing can be usually achieved by simply characterizing the specific changes in absorbance or fluorescence signal caused by enzyme-catalysed substrates or products, whereas electrochemical biosensing is typically realized by coupling a modified electrode (i.e. using enzyme-loaded-mesophase) with an electrochemical detection device.¹¹⁻¹⁵ These highly sensitive analyte-specific biosensing systems can be used to detect numerous analytes such as glucose (glucose oxidase - GOx), toxic phenolic compounds and hydrogen peroxide (horseradish peroxidase - HRP).

In comparison with the other gel-like biosensor matrices (i.e. hydrogels and sol-gels), lipid-based cubic phases offer several unmatched advantages. First, they have the intrinsic capacity to retain their structural features at thermodynamic equilibrium with a surrounding environment of excess water, which makes them ideal candidates for the design of reusable

electrochemical biosensors.¹¹⁻¹⁶ Secondly, these highly curved 3D periodic liquid crystalline structures, which have been observed in numerous types of stressed or virally infected cells,²⁰ are biomimetic and can therefore provide an enzyme environment quite similar to that found under *in-vivo* conditions, where the surrounding solutions are usually not homogeneous and enzymes attach to cellular structures, i.e. membrane bilayers. Therefore, apart from the potential as biosensors, the enzymatic activity study in cubic phases can also provide invaluable insights towards the enzyme kinetics in biological systems.

Recently, Li and Caffrey,²¹ and Zabara *et al.*²² have shown the successful reconstitution of an integral membrane enzyme and pore-forming transmembrane protein, respectively, into bicontinuous cubic phases and moreover demonstrated that the reconstituted proteins were capable of retaining their specific functionalities. Yet, although great progresses have been made on understanding the specific interactions occurring within protein-loaded mesophases as well as their potential use in real-life applications, these distinct hosting media also present a number of drawbacks. One of the most limiting factors of the bicontinuous cubic phase lies with the relatively small diameter of its aqueous channels (typically smaller than 4 nm), which not only hinders the mobility of the encapsulated enzymes (i.e. GOx $D_h \sim 8\text{nm}$; HRP $D_h \sim 6\text{nm}$), but also forces the enzyme molecules within a highly confined architecture, hampering their full enzymatic activity. To this point, Nylander *et al.*¹¹ previously reported that within the same mesophase, smaller enzymes can keep their relative activity for longer periods of time and, implicitly, that the enzyme size can directly determine their long-term stability inside the mesophase. Fortunately, this limitation can be overcome by including hydration-modulating surfactants (such as octyl glucoside, sucrose stearate and polyglycerol ester)²³⁻²⁸ into the host lipid (monoglyceride) resulting in a significant increase of their hydrophilic domains. Consequently, the water channels diameters of bulk cubic phases can be tuned in a highly controlled and reproducible way, by simply adjusting the added amount of hydration-

enhancing agent. These specially designed swollen mesophases provide a significantly improved environment for the encapsulated enzymes, not only by removing the spatial constraints of the protein molecules but also by allowing much faster diffusion of other relevant molecules^{9,26} (i.e. substrate or products).

In the present study, using horseradish peroxidase (HRP) as a model protein system, we systematically characterized the activity and kinetics of this enzyme within bulk mesophases, correlating for the first time its *in-meso* activity with the water channel sizes of the hosting mesophases. In all experiments the enzyme was found to be in a functionally active form, although the enzymatic activity was significantly lower in the case of the standard mesophase (water channel diameter $D = 3.5$ nm). The addition of hydration-enhancing surfactants to the mesophase, resulted in a significant increase of the water channel size ($D = 7.2$ nm), and the resulting enzymatic activity was greatly preserved: compared to ‘standard mesophase’ the enzymatic activity was more than double in the swollen mesophase, approaching that in bulk free water. In these experiments, the enzyme was physically immobilized and the substrates were solubilized in the water channels in order to ensure that the enzymatic reaction takes place homogeneously within the bulk mesophases. Thus, this approach differs substantially from all of the earlier studies where the enzymatic activity in presence of mesophases is explored in excess water conditions. Although in the long run the present approach may cause accumulation of enzymatic products inside the mesophases, it overcomes the inevitable differentials between the operational enzymatic reaction rates and the real reaction rates induced by the osmotic stresses and concentration gradients typically occurring in the case of excess water conditions.²¹ Our study aims at better understanding the role of physical confinement on *in-meso* enzymatic reactions and can lead to a significant improvement in the future developments of analyte-specific biosensors.

Materials and Methods

Materials. Dimodan U/J (Danisco, Denmark, Batch Number 015312), a commercial-grade of monoglyceride ($\geq 90\%$), was used as received. Sucrose stearate S-1670 (SE), a blended sugar ester (75% of monoester and 25% of di-, tri- and polyesters), was a gift from Mitsubishi-Kagaku Foods Corporation, Japan. Horseradish peroxidase (HRP, lyophilized, powder, ~ 150 U/mg), 2,2'-Azino-bis(3-ethylbenzothiazoline-6-sulfonic acid) diammonium salt (ABTS, 98.0%), hydrogen peroxide (50% H_2O_2 in H_2O), phosphate buffer (PBS, pH = 7.0) and acetate buffer (pH = 4.65) were purchased from Sigma-Aldrich.

Small-angle X-ray scattering. The symmetry of the various mesophases was identified by Small-angle X-ray scattering (SAXS, Rigaku MicroMax-002+ microfocussed X-ray source operating at 45 kV and 88 mA). The Ni-filtered Cu $K\alpha$ radiation ($\lambda = 1.5418 \text{ \AA}$) was collimated by three pinholes of 0.4, 0.3 and 0.8 mm, respectively and the scattered intensity was collected by a 2D argon-filled Triton-200 X-ray detector (20 cm diameter, 200 μm resolution) for over 30 min. The scattering vector is defined as $q = 4\pi \sin(\theta)/\lambda$ with a scattering angle 2θ and q was calibrated using silver behenate. The effective scattering vector ranged from 0.01 \AA^{-1} to 0.44 \AA^{-1} . The semisolid gel-like mesophase samples were placed on a Linkam hot stage between two mica sheets spaced by a 1 mm O-ring. For all our SAXS measurements, the temperature was controlled at $37 \text{ }^\circ\text{C}$.

Phase Diagram. Polarized microscopy was used as a rapid screen to rule out the presence of birefringent mesophases (lamellar phase (L_a) possibly coexisting with the isotropic background (constituted by the bulk cubic phase). Small-Angle X-ray scattering was used to refine the phase diagram and extract topological information. All these phase behaviors were studied at $37 \text{ }^\circ\text{C}$ with PBS buffer (10 mM PO_4^{3-} /150 mM NaCl, pH = 7.0) to be fully consistent with the enzymatic studies investigated in buffer conditions at $37 \text{ }^\circ\text{C}$.

Sample Preparation for Enzymatic Studies. A setup²⁹ composed of two connected Hamilton RN syringes was used to prepare the mesophase samples. To prepare pure mesophases without enzyme and substrates inside, we loaded one syringe with monoglyceride (M) or monoglyceride-SE (M-SE) mixtures and the other with Acetate Buffer (pH=4.65), then we mixed them until the blend was totally homogeneous. To prepare the mesophase samples with enzyme and substrates for the enzymatic activity studies, the desired amount of HRP solution (dissolved in PBS buffer pH = 7) was loaded with M or M-SE mixtures in one syringe while the other syringe was loaded with the substrate ABTS and the H₂O₂-containing Acetate Buffer (pH=4.65). Following this procedure, the enzymatic reaction cannot start until the mixing of the two syringe loads is operated. Since the enzymatic reaction within the mesophase typically presents an initial lag period, we paid particular attention to finalize mixing well within the lag period, and to operate the mixing step within a constant time. Therefore, analysis of the lag period at different swollen conditions is simply affected by a constant offset. It should be emphasized that in all enzymatic activity studies presented in this work, the water content is always close, but below maximum hydration, ensuring that the enzymatic reactions takes place in bulk.

UV-vis Spectroscopy. The mesophases with enzyme and substrate were transferred from the Hamilton RN syringe to a demountable closed cuvette (Starna GmbH). The kinetic mode of the Cary 100 Bio UV-vis spectrophotometer was employed to record all the progress curves of HRP enzymatic reactions at a fixed wavelength of 418 nm at 37 °C. From the evolution of the absorption curves the enzyme activity and kinetics were calculated.

Results and discussion

SE Induces Swollen Cubic Mesophases. In the usual monoglyceride-water binary phase diagram,³⁰ the Pn3m water channel diameter can only be increased up to a maximum of about 3.6 nm. No more than 35% water can be incorporated inside the water channel of the bulk

Pn3m. However, when the hydration-enhancing agent SE is added to the monoglyceride-water system, a significant shift in the phase boundaries and location of the Pn3m cubic phase was observed. The detailed phase behavior of the ternary monoglyceride-SE-water system at 37 °C is given in Fig. 1a. The presence of the hydration-enhancing surfactant leads to a different phase behavior where more than 52% water can be partitioned inside the bulk mesophase resulting in a significant increase in the water channel diameter, up to a maximum of 7.2 nm, calculated as previously described.^{26,27} We note here, that the PBS buffer (10 mM PO₄³⁻/150 mM NaCl) used, results in the preservation of the Pn3m cubic phase up to maximum hydration, without transition to the Im3m cubic phase, as previously reported with Milli-Q water in our earlier work.²⁶

In order to explore the possibility of fine-tuning the structural properties of host mesophase we prepared a range of Pn3m cubic phases with increasing amount of SE, 0%, 10%, 15%, 20% and water content just below maximum hydration, as shown in Figure 1b (Figure S2, 2D graph). By comparison of Figure 1b and 1c, we can obviously see that the water channel size of the swollen Pn3m containing 20% SE (7.2 nm) is more than double of that of standard Pn3m (3.5 nm) without SE.

The largest water channel diameter of the swollen Pn3m is above the HRP hydrodynamic diameter (~6 nm), which, together with the increased lipid membranes flexibility, provides bulk-like conditions for the enzyme activity compared to the highly confined case offered by the standard cubic phase. In order to test this hypothesis we performed a systematic enzymatic activity study in the four Pn3m cubic phases obtained by increasing SE, that is, with increasing water content/channel diameters.

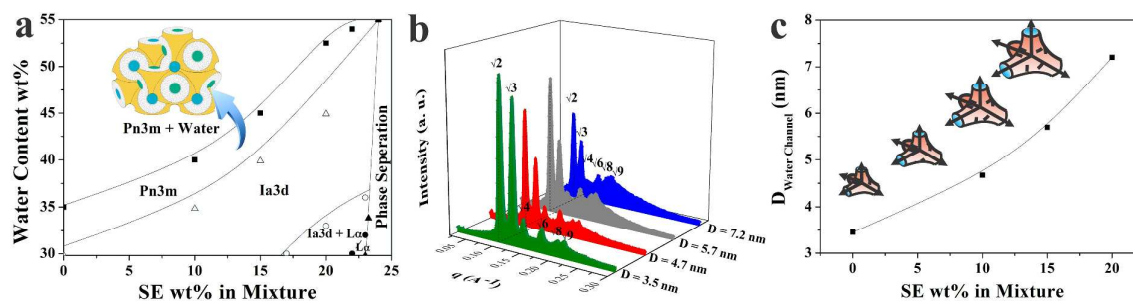


Figure 1. a) Phase diagram of the monoglyceride/SE-water ternary system, as obtained by polarized optical microscope and SAXS. b) 1D SAXS spectra of scattered intensities vs. scattering vector q , showing four Pn3m phases with increasing amount of SE 0%, 10%, 15% and 20% (from front to back) at water content 33%, 40%, 45%, 52%, which are all just below maximum hydration. The Pn3m phase symmetry was identified via the specific spacing of the reflection peaks following the ratio $\sqrt{2}:\sqrt{3}:\sqrt{4}:\sqrt{6}:\sqrt{8}:\sqrt{9}$. c) Corresponding increase in water channel diameter of the SE-monoglyceride-water Pn3m mesophase as a function of increasing SE content at water content just below maximum hydration (33%, 40%, 45%, 52%, respectively).

HRP Activities in the Standard Mesophase, Swollen Mesophases and Bulk Water. In order to gain a better understanding on the interplay between spatial confinement and enzymatic activity, we have performed several enzymatic activity studies in various *in-meso* environments, while maintaining identical final enzyme and enzymatic reactant concentrations: [HRP] = 0.003 mg/mL, ABTS = 2 mM, H₂O₂ = 20 mM (all concentrations shown are in water, see Figure S3 for the small ABTS partition coefficient). To start, using UV-vis spectroscopy (Figure 2a), we demonstrate that HRP is catalytically active in the bicontinuous cubic phase. Comparing the progress curves in Figure 2a, one can immediately note that by increasing the hydration (right to left), the reaction curve of the HRP enzymatic

transformation gets progressively steeper, indicating faster enzymatic reaction in swollen mesophases.

For most enzymes, including our model enzyme HRP in bulk water conditions, the initial reaction rates are the maximal rates without any latency. However, in the progress curves of enzyme reaction within mesophases (Figure 2a), an initial period (the so-called latency or lag period) can be clearly observed with no significant activity, before a detectable linear reaction regime starts (the slope defined as the initial rate value). This lag behaviour has already been recognized and discussed in early studies.³¹⁻³⁴ With respect to *in-meso* studies, a lag period for the enzymatic activity of diacylglycerol kinase was observed by Caffrey *et al.*²¹ Although the enzyme activation process is taken as a common reason for the lag period,^{31,32} it has also been shown that restricted substrate accessibility can be another possible source for appearance of a lag time.^{33,34} In our case the *in-meso* lag period is tentatively attributed to the restricted diffusion of the substrate molecules *in-meso*, slowing down their access to the active sites of the physically immobilized enzymes. Strong further evidence in support of this hypothesis is that the lag period time was found to decrease with the increasing mesophase water channel size (Figure 2b), which is again consistent with our previous report²⁶ that the diffusion coefficient increased with the swelling of the water channel.

In all cases, the initial rates of enzyme reactions were extracted via linear regression of the early portions of the progress curves (see Figure S4 for a zoom-up of the enzymatic reaction in pure bulk water). Figure 3a and 3b rationalize the relationship between enzyme initial reaction rates (Figure 3a) and relative activity (Figure 3b) versus water channel size. The initial rate of reaction increases exponentially while the relative activity increases linearly with increasing water channel sizes. With the swelling of water channels (decrease of the ratio between the diameter of the enzyme and that of the water channels, $D_{\text{enzyme}}/D_{\text{water channel}}$), the

enzymatic activities plateau-off and approaches the characteristic values of unrestricted enzymatic reaction in water when $D_{\text{water channel}} \rightarrow \infty$ (i.e. $D_{\text{enzyme}}/D_{\text{water channel}} \rightarrow 0$).

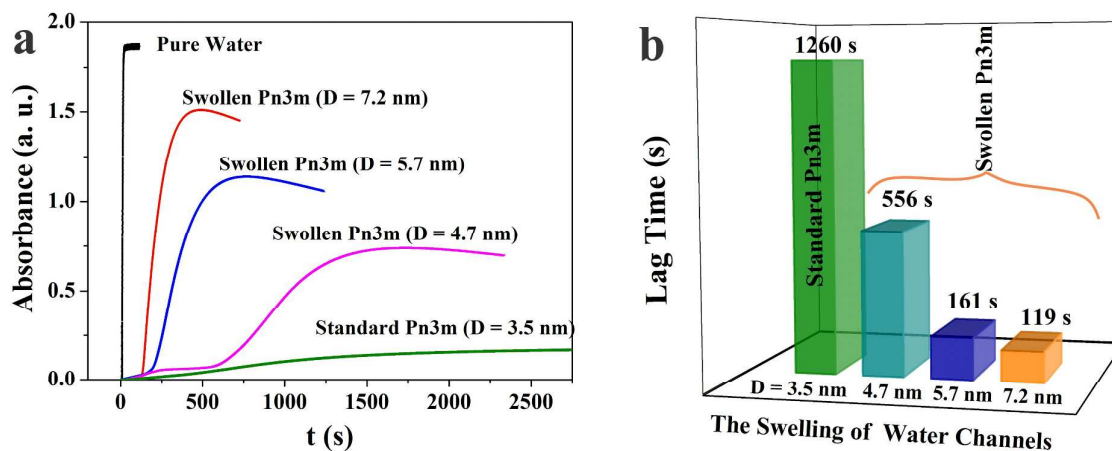


Figure 2. a) Progress curves of HRP enzymatic reaction with $[HRP] = 0.003 \text{ mg/mL}$, $ABTS = 2 \text{ mM}$, and $H_2O_2 = 20 \text{ mM}$ within pure water, standard Pn3m (monoglyceride alone with 33% water, $D = 3.5 \text{ nm}$) and three differently swollen Pn3m mesophases: monoglyceride:SE 90:10 with 40% water ($D = 4.7 \text{ nm}$), monoglyceride:SE 85:15 with 45% water ($D = 5.7 \text{ nm}$) and monoglyceride:SE 80:20 with 52% water ($D = 7.2 \text{ nm}$). (b) Lag time decrease with the swelling of the water channels.

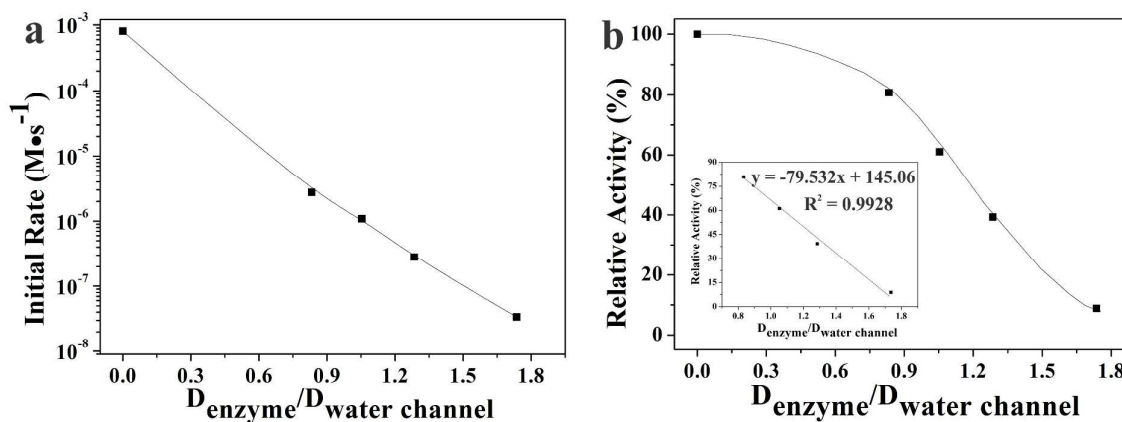


Figure 3. Semi-log plot of initial reaction rate (a) and linear plot of relative activity (b) versus the water channel size, expressed via $D_{enzyme}/D_{water\ channel}$; the relative activity shows a linear dependency on water channel sizes (b, inset). The initial reaction rate and relative activity values are calculated from the UV progress curves shown in Figure 2a.

In-meso Enzymatic Kinetics in Standard vs Swollen Mesophases. In order to follow the *in-meso* kinetics of the catalytic HRP enzyme reaction $ABTS + H_2O_2 \xrightarrow{HRP} oxidized\ ABTS + H_2O$, the enzyme concentration were kept constant within each specific environment; however, for varying confinement environments, the enzyme concentration was let change to allow recording the enzymatic reactions at varying ABTS concentrations (Figure S5). It should also be mentioned that the amount of hydrogen peroxide used was saturated for the enzyme kinetics, yet maintained in limited excess, because although higher H_2O_2 concentration has no influence on the symmetry of the host mesophases (Figure S6), it can cause over oxidation and backward reaction (Figure S8), as previously reported for enzymatic reactions carried out in the gel phase.³⁵

Conventionally, the Michaelis-Menten equation is taken as a model to describe enzymatic kinetics, taking the initial rate of reaction v , as a function of substrate concentration $[s]$:³⁶

$$v = \frac{V_{max}}{K_m + [s]} [s] \quad (1)$$

where K_m and V_{max} are the Michaelis-Menten constant and the maximum velocity, respectively, which can be both obtained by fitting the enzymatic kinetics curves. These two kinetics parameters determine the initial catalysis rate of enzyme at a certain substrate concentration.

Michaelis-Menten kinetics is well suited to describe the kinetics of free enzymes in homogeneous solutions *in vitro*. In a few cases, immobilized enzymes have also been shown to follow a Michaelis-Menten kinetics,³⁷⁻³⁹ and a Michaelis-Menten behavior was even reported for the membrane enzyme diacylglycerol kinase in bicontinuous cubic phases.²¹ However, it has already been theoretically predicted⁴⁰⁻⁴² and experimentally observed^{43,44} that when enzymes are immobilized, their kinetic properties would deviate from Michaelis-Menten kinetics and to show a typical sigmoidal behaviour.

Here we found, for the first time *in-meso*, that the enzymatic kinetics of HRP (Figure 4) shows a sigmoidal behaviour with significant deviations from the Michaelis-Menten model. Since the Michaelis-Menten model is only applicable to describe reaction-controlled enzyme reaction kinetics, as in bulk water conditions,⁴⁰⁻⁴⁴ diffusion-controlled kinetics is likely to be better interpreted by the more general Hill model, which has been applied to describe the kinetics of enzymes exhibiting substantial deviations from the Michaelis-Menten model:⁴⁵⁻⁴⁷

$$v = \frac{V_{max}}{K_m^n + [s]^n} [s]^n \quad (2)$$

Thus, the Hill model is a generalization of the Michaelis-Menten model allowing n larger or smaller than 1, and reverts back to the Michaelis-Menten model when n equals 1.

By fitting progress curves with the Hill model, we obtain K_m , V_{max} and n values, from which the turnover number K_{cat} ($K_{cat} = V_{max}/[E]$, with $[E]$ the enzyme concentration) and the catalytic efficiency K_{cat}/K_m can be calculated. These enzyme kinetics parameters are shown in Table 1 for the different mesophases and bulk water solutions.

Comparing the enzymatic kinetics parameters in Table 1, a clear picture emerges: the K_m values of HRP increase steadily from pure water to the swollen Pn3m mesophase (monoglyceride:SE 80:20 with 52% water) to the normal Pn3m mesophase (monoglyceride alone with 33% water). The lower the K_m value is, the higher the affinity between the enzyme

and the substrate is. K_{cat} and K_{cat}/K_m follow the opposite trend, being at maximum in the pure water case, decreasing in the swollen Pn3m and decreasing further in the standard Pn3m cubic phase. Interestingly, the turnover number of HRP within the swollen Pn3m cubic phase maintains 92.1% of the corresponding value in pure water solution, while being 2.6 times larger than the corresponding value in the standard Pn3m cubic phase (35.2%).

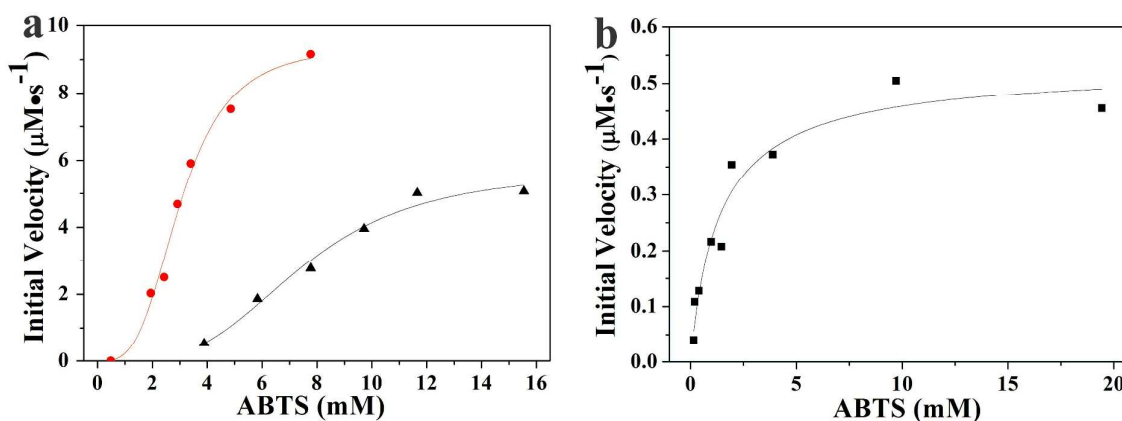


Figure 4. Enzymatic kinetics curves of HRP in three different environments: swollen Pn3m cubic phase (M:SE 80:20 with 52% water - Figure 4a red circles); standard Pn3m cubic phase (M alone with 33% water - Figure 4a black triangles); pure water solution (b). The HRP concentration is 0.006 mg/mL, 0.009 mg/mL, 0.0003 mg/mL, respectively.

Table 1. The enzymatic kinetics parameters of HRP as obtained from Hill model in the three environments considered in this work: bulk water, swollen Pn3m and standard Pn3m mesophase.

Kinetics parameters	Pure water	Swollen Pn3m	Standard Pn3m
K_m (mM)	1.4	3.0	7.5
n	0.9	3.3	3.4
K_{cat} (s^{-1})	78.4	72.2	27.6
$K_{cat}/K_{cat\ water}$	100%	92.1%	35.2%
K_{cat}/K_m ($mM^{-1}\cdot min^{-1}$)	55.6	23.9	3.7

Taken together, all the above results indicate that swollen Pn3m cubic phases provide a much more suitable environment for the enzyme to react compared to the standard Pn3m mesophases, approaching kinetics parameters typical of enzymatic reaction in pure water, although differences from the unrestricted kinetics in pure water environment remain noticeable in all mesophase cases, such as, for example, in the Hill coefficient n , which maintains values higher than 1.

These results can be understood by considering the highly confined environment offered by the mesophases for the *in-meso* enzymatic reaction. The water channels diameter of the standard Pn3m is calculated to be 3.5 nm, far smaller than the HRP diameter (~6 nm). Although the unperturbed Pn3m bicontinuous cubic phase lipid bilayers are flexible and the water channels have the capacity to expand when enzymes are loaded, the expansion is energetically unfavorable.^{48,49} The deformation energy for the inclusion of the HRP enzyme within the standard cubic phases estimated by the Helfrich theory of curvature elasticity⁴⁸ can be of the order of decades of $k_B T$, in agreement with the energetic penalty estimation for

nanoparticles of similar sizes within lipid-based lyotropic liquid crystals.⁴⁹ Furthermore, SAXS results in Figure S7a indicate that the water channel size of the standard Pn3m remained unchanged after different concentrations of enzymes were loaded. This suggests two possible scenarios: i) either the enzyme molecules did not enter the water channels, remaining confined and immobilized within the mesophase grain boundaries, or ii) they did enter, but the structure of the enzymes was altered accordingly, implying protein unfolding. Therefore, both enzyme immobilization and partial unfolding, or a combination thereof, together with the reduced diffusion rate of the substrate in the standard mesophase can be advanced as possible causes of the huge reduction of the enzymatic activity and the sigmoidal kinetic behaviour of the HRP *in-meso*.

In contrast, when the water channel diameter of the cubic phase is increased beyond the size of the enzyme, i.e. to 7.2 nm, HRP can freely diffuse and enter within all aqueous domains of the mesophases, reducing its unfolding/immobilization-induced inactivation, which, together with the increased diffusion of the substrate, results again in a kinetic behaviour reminiscent of that observed in free water: in this case the sigmoidal profile is nearly entirely smeared and enzymatic turnover number differs by only 8% from that measured in pure water. Figure 5 summarizes the rationale and the main findings discussed above.

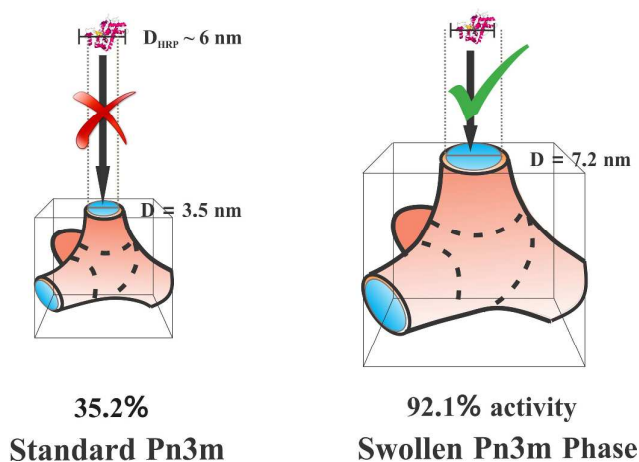


Figure 5. Schematic illustration of HRP in the unperturbed Pn3m (monoglyceride alone with 33% water, left) and the swollen Pn3m bicontinuous cubic phases (monoglyceride:SE 80:20 with 52% water, right).

Conclusions

We have systematically investigated the effect of the release of the physical nano-confinement on the enzymatic activity of horse-radish peroxidase, a model hydrophilic enzyme, dispersed within lipidic bicontinuous cubic phases of double diamond Pn3m space group symmetry.

The level of confinement was controlled by blending to the monoglyceride lipids, sugar ester surfactants as hydration enhancing agents, allowing an increase by more than 100% in the diameter of the mesophase water channels, while preserving the symmetry of the liquid crystals. This corresponded to water channels diameter either smaller or larger than the enzyme diameter, in the unperturbed and swollen mesophases, respectively.

Although the enzymes were found to be in functionally active state in all cases, the *in-meso* enzymatic activity was significantly decreased within the standard mesophase, while a nearly three-fold larger enzymatic activity was observed in the swollen mesophase. A restricted-diffusion-induced initial lag period was exhibited by the physically-entrapped enzymes *in-meso* and found to decrease upon swelling. Moreover, the enzymatic kinetics of the horse-radish peroxidase in the confined mesophase environment was shown to deviate substantially from the Michaelis-Menten behaviour expected for free enzymes kinetics, and to be better interpreted by the more general Hill function. In particular, the Hill coefficients were showed to approach a Michaelis-Menten behaviour upon release of the confinement by swelling the mesophase to water diameters beyond the enzyme size.

We interpret these results in terms of the partial inactivation/immobilization of the enzyme upon the increased nanoconfinement within the mesophase, which is accompanied by the diffusion-restricted accessibility of the substrates to enzymes. The kinetics of freely diffusing native enzyme can be restored by releasing the nanoconfinement upon mesophase swelling, asymptotically approaching a kinetic fingerprint typical of horse-radish peroxidase in free bulk water. These findings push considerably forwards the current understanding of the interplay between the physical confinement and the activity of enzyme molecules dispersed in nanostructured heterogeneous fluids.

Acknowledgements: The authors gratefully acknowledge the China Scholarship Council and ETH Zurich for the financial support of this work. Renata Negrini (ETH Zürich) is kindly acknowledged for valuable discussions on the swollen mesophase phase behaviours.

Notes and references:

*ETH Zurich, Food and Soft Materials Science, Institute of Food, Nutrition & Health,
Department of Health Science and Technology, Schmelzbergstrasse 9, CH-8092 Zurich,
Switzerland.*

** To whom correspondence should be addressed: Email: raffaele.mezzenga@hest.ethz.ch*

† Electronic Supplementary Information (ESI) available: [Visual appearance of the standard mesophase before and after HRP enzymatic reaction (Figure S1); SAXS results of four Pn3m phases with increasing amount of SE 0%, 10%, 15% and 20% just below maximum hydration (Figure S2); calibration curve for determining the partition coefficient of ABTS in lipids (Figure S3); progress curves of the HRP catalytic reaction in pure water (Figure S4) and reactions at varying ABTS concentrations for the in-meso enzymatic kinetics studies (Figure S5); SAXS characterization of the influence of the added H₂O₂ (Figure

S6) and HRP (Figure S7) on the hosted mesophases; initial rate as function of H₂O₂ concentration in 3 varying environments (Figure S8)]. See DOI: 10.1039/b000000x/

1. J. Clogston and M. Caffrey, *J. Control Release*, 2005, **107**, 97–111.
2. W. Fong, T. Hanley and B. Boyd, *J. Control Release*, 2009, **135**, 218–226.
3. R. Negrini and R. Mezzenga, *Langmuir*, 2011, **27**, 5296–5303.
4. F. Caboi, T. Nylander, V. Razumas, Z. Talaikytė, M. Monduzzi and K. Larsson, *Langmuir*, 1997, **13**, 5476–5483.
5. I. Amar-Yuli, D. Libster, A. Aserin and N. Garti, *Curr. Opin. Colloid Interface Sci.*, 2009, **14**, 21–32.
6. B. Angelov, A. Angelova, B. Papahadjopoulos-Sternberg, S. V. Hoffmann, V. Nicolas and S. Lesieur, *J. Phys. Chem. B*, 2012, **116**, 7676–7686.
7. V. Cherezov, D. M. Rosenbaum, M. A. Hanson, S. G. Rasmussen, F. S. Thian, T. S. Kobilka, H. J. Choi, P. Kuhn, W. I. Weis, B. K. Kobilka and R. C. Stevens, *Science*, 2007, **318**, 1258–1265.
8. M. Caffrey and V. Cherezov, *Nat. Protoc.*, 2009, **4**, 706–731.
9. A. Zabara and R. Mezzenga, *Soft Matter*, 2012, **8**, 6535–6541.
10. P. V. Braun and S. I. Stupp, *Mater. Res. Bull.*, 1999, **34**, 463–469.
11. V. Razumas, J. Kanapienienė, T. Nylander, S. Engström and K. Larsson, *Anal. Chim. Acta.*, 1994, **289**, 155–162.
12. T. Nylander, C. Mattisson, V. Razumas, Y. Mieziš and B. Håkansson, *Colloid Surfaces A*, 1996, **114**, 311–320.
13. E. Nazaruk and R. Bilewicz, *Bioelectrochemistry*, 2007, **71**, 8–14.
14. E. Nazaruk, R. Bilewicz, G. Lindblom and B. Lindholm-Sethson, *Anal Bioanal Chem.*, 2008, **391**, 1569–1578.

15. E. Nazaruk, E. Górecka and R. Bilewicz, *J. Colloid Interface Sci.*, 2012, **385**, 130–136.
16. A. Angelova, M. Ollivon, A. Campitelli and C. Bourgaux, *Langmuir*, 2003, **19**, 6928–6935.
17. H. K. Kim, S. Y. Lim, D. H. Nam, J. Ryu, S. H. Ku and C. B. Park, *Biosens. Bioelectron.*, 2011, **26**, 1860–1865.
18. V. Vamvakaki and N. Chaniotakis, *Biosens. Bioelectron.*, 2007, **22**, 2650–2655.
19. W. Jia, K. Wang, Z. Zhu, H. Song and X. Xia, *Langmuir*, 2007, **23**, 11896–11900.
20. Z. Almsherqi, S. Kohlwein and Y. Deng, *J. Cell Biol.*, 2006, **173**, 839–844.
21. D. Li and M. Caffrey, *Proc. Natl. Acad. Sci.*, 2011, **108**, 8639–8644.
22. A. Zabara, R. Negrini, O. Onaca-Fischer and R. Mezzenga, *Small*, 2013, **9**, 3602–3609.
23. B. Angelov, A. Angelova, M. Ollivon, C. Bourgaux and A. Campitelli, *J. Am. Chem. Soc.*, 2003, **125**, 7188–7189.
24. B. Angelov, A. Angelova, V. Garamus, G. Lebas, S. Lesieur, M. Ollivon, S. Funari, R. Willumeit and P. Couvreur, *J. Am. Chem. Soc.*, 2007, **129**, 13474–13479.
25. A. Angelova, B. Angelov, R. Mutafchieva, S. Lesieur and P. Couvreur, *Acc. Chem. Res.*, 2011, **44**, 147–156.
26. R. Negrini and R. Mezzenga, *Langmuir*, 2012, **28**, 16455–16462.
27. R. Negrini and R. Mezzenga *Langmuir*, 2013, **29**, 1327.
28. A. Chemelli, M. Maurer, R. Geier and O. Glatter, *Langmuir*, 2012, **28**, 16788–16797.
29. A. Cheng, B. Hummel, H. Qiu and M. Caffrey, *Chem. Phys. Lipids*, 1998, **15**, 11–21.
30. R. Mezzenga, C. Meyer, C. Servais, A. Romoscanu, L. Sagalowicz and R. Hayward, *Langmuir*, 2005, **21**, 3322–3333.
31. E. B. Kearney, *J. Biol. Chem.*, 1957, **229**, 363–375.
32. A. D. Bangham and P. M. C. Dawson, *Biochem. J.*, 1959, **72**, 486–492.
33. R. P. Sandstrom, L. L. Terri and E. C. Robert, *Plant Physiol.*, 1987, **85**, 693–698.

34. G. Basáñez, J-L. Nieva, F. M. Goñi and A. Alonso, *Biochemistry.*, 1996, **35**, 15183-15187.
35. E. Kadnikova and N.Kostić, *J. Mol. Catal. B: Enzym.* 2002, **18**, 39–48.
36. L. Michaelis and M. Menten, *Biochem. Z.*, 1913, **49**, 333-369.
37. A. Blandino, M. Macías and D. Cantero, *Process Biochem.*, 2001, **36**, 601-606.
38. G. Zhen, V. Eggli, J. Vörös, P. Zammaretti, M. Textor, R. Glockschber and E. Kuennemann, *Langmuir*, 2004, **20**, 10464-10473.
39. G. Wang, J. Xu, H. Chen and Z. Lu, *Biosens. Bioelectron.*, 2003, **18**, 335-343
40. J-M. Engasser and C. Horvath, *J. Theor. Biol.*, 1973, **42**, 137-155.
41. J-M. Engasser and C. Horvath, *Biochem. J.*, 1975, **145**, 431-435.
42. J. Vincent and M. Thellier, *Biophys. J.*, 1983, **41**, 23-28.
43. S. Vishvanath, D. Bhattacharyya, W. Huang and L. Bachas, *J. Membr. Sci.*, 1995, **108**, 1-13.
44. B. Lakard, G. Herlem, S. Lakard, A. Antoniou and B. Fahys, *Biosens. Bioelectron.*, 2004, **19**, 1641-1647.
45. J. Ricard and A. Cornish-Bowden, *Eur. J. Biochem.*, 1987, **166**, 255-272.
46. K. Helmstaedt, S. Krappmann and G. Braus, *Microbiol. Mol. Bio. Rev.*, 2001, **65**, 404-421.
47. B. Bunow, *J. theor. Biol.* 1980, **84**, 611-627.
48. W. Helfrich, *Z. Naturforsch.* 1973, **28c**, 693-703.
49. E. Venugopal, S. Bhat, J. J. Vallooran and R. Mezzenga, *Langmuir*, 2011, **27**, 9792-9800.

Graphical abstract

